EPJ Web of Conferences **26**, 04032 (2012)
DOI: 10.1051/epjconf/20122604032

Fragmentation of armor piercing steel projectiles upon oblique perforation of steel plates

V. Paris, A. Weiss, A. Vizel, E. Ran, and F. Aizik

Plasan Sasa Ltd. Kibbutz Sasa, M.P. Merom Hagalil 13870, Israel

Abstract. In this study, a constitutive strength and failure model for a steel core of a14.5 mm API projectile was developed. Dynamic response of a projectile steel core was described by the Johnson-Cook constitutive model combined with principal tensile stress spall model. In order to obtain the parameters required for numerical description of projectile core material behavior, a series of planar impact experiments was done. The parameters of the Johnson-Cook constitutive model were extracted by matching simulated and experimental velocity profiles of planar impact. A series of oblique ballistic experiments with x-ray monitoring was carried out to study the effect of obliquity angle and armor steel plate thickness on shattering behavior of the 14.5 mm API projectile. According to analysis of x-ray images the fragmentation level increases with both steel plate thickness and angle of inclination. The numerical modeling of the ballistic experiments was done using commercial finite element code, LS-DYNA. Dynamic response of high hardness (HH) armor steel was described using a modified Johnson-Cook strength and failure model. A series of simulations with various values of maximal principal tensile stress was run in order to capture the overall fracture behavior of the projectile's core. Reasonable agreement between simulated and x-ray failure pattern of projectile core has been observed.

1 Introduction

Armor piercing projectiles made of high carbon hardened steel are good penetrators of steel armor at normal incidence. However, they are known to be susceptible to shattering at oblique perforation of armor steel plates. Yeshurun et al. [1] found that 4 mm high hardness steel plates at obliquities higher than 45 degrees have a very high ballistic efficiency against both 0.5″ and 14.5 mm armor piercing (AP) projectiles. Upon oblique impact, the projectile is subjected to asymmetric loading that leads to the propagation of bending waves along the projectile and finally results in multiple brittle fractures of the core. The possibility of effective use of oblique impact in armor design provides a firm motivation to investigate the issue both experimentally and numerically. Reliable numerical simulation of oblique impact requires a material model able to capture the effect that obliquity has on the fragmentation behavior of the AP projectile. This is a major issue addressed in the present study.

A series of oblique ballistic experiments with x-ray monitoring was carried out to study the effect of obliquity angle and armor steel plate thickness on shattering behavior of the 14.5 API projectile. According to analysis of x-ray images, the fragmentation level increases with both steel plate thickness and angle of inclination. The numerical modeling of the ballistic experiments was done using commercial finite element code, LS-DYNA. Dynamic response of the projectile steel core was described by the Johnson-Cook constitutive model combined with the principal tensile stress fracture criterion. In order to obtain the parameters required for numerical description of projectile core material behavior, a series of planar impact experiments was done. The parameters of the Johnson-Cook constitutive model were extracted by matching the planar impact results. A series of simulations with various values of principal tensile stress was run in order to capture the overall fracture behavior of the projectile's core. Reasonable agreement between the simulated and x-ray failure pattern of the projectile core has been observed.

2 Materials and planar impact tests

The 14.5 mm armor piercing projectile (14.5API BZ32 RU) is comprised of a hardened steel core and steel jacket and incendiary powder. The core is made of high carbon content (1.3% wt.) steel and is hardened to Vickers hardness of ~900 VHN.

Two planar impact tests with samples cut from the core of the 14.5 mm AP projectile were carried out in order to characterize high-strain-rate strength of the core material. The experiments were done using a 58-mm bore diameter gas gun to accelerate the sabot with impactor disk. The Velocity Interferometer System for Any Reflector (VISAR) [2] was used for measurement of the sample free surface velocity. Details of these tests are given in Table 1 while details of the experimental facility may be found in [3]. The velocity histories recorded in planar impact experiments, BALA and BALB, are presented in Figure 1. Analysis of the recorded velocity histories reveals that velocity amplitude corresponding to the Hugoniot elastic limit (HEL) of the core steel is ~ 100 m/s. The stress at HEL, σ_{HEL} =~2.3 GPa, was calculated with the aid of Eq. (1),

$$\sigma_{HEL} = 1/2\rho_0 C_L u_{HEL}, \quad (1)$$

where: ρ_0 is the initial material density, C_L is the longitudinal sound speed and u_{HEL} is the velocity amplitude at HEL.

The HEL is hardly distinguishable because of the subsequent strong strain hardening and strain rate hardening of the material. From the stress at HEL the dynamic yield stress, Y_D, may be obtained using Eq. (2),

$$Y_D = \sigma_{HEL}(1 - 2\nu)/(1 - \nu), \quad (2)$$

Table 1. Details of planar impact tests.

Test #	BALA	BALB
Sample thickness (mm)	3.10	3.87
Impactor thickness (mm)	1.0	1.0
Impactor material	Copper	Tungsten
Impact velocity (m/sec)	600	623

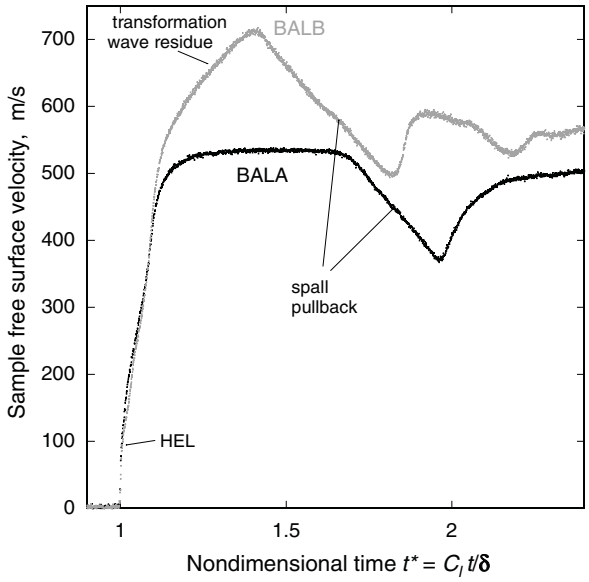

Fig. 1. VISAR- recorded free surface velocity histories of planar impact tests with samples of the 14.5API core. The abscissa here is a non-dimensional time defined as normal time multiplied by longitudinal sound speed C_l and divided by sample thickness δ.

where: ν is Poisson's ratio. Equation (2) yields about 1.35 GPa for dynamic yield stress, Y_D. Apparently, in the stronger planar impact test BALB phase transformation ($\alpha \rightleftarrows \varepsilon$) of the steel occurred [4]. This is manifested in the upper portion of the velocity history. The spall strength was calculated according to the measured velocity pullback, using Eq. (3):

$$\sigma_{spall} = 1/2\rho_0 C_0 u_{pb} \tag{3}$$

where: ρ_0 is the initial material density, C_0 is bulk sound speed and u_{pb} is the velocity spall pullback. The spall strength is 3 and 3.8 GPa for BALA and BALB tests, respectively. The spall strength for the BALB test calculated using Eq. (3) has some additional uncertainty due to $\alpha \rightleftarrows \varepsilon$ phase transition. The higher value of the spall strength in the BALB test may be attributed to the phase transformation of the material [5] although the contribution of the strain rate effect cannot be ruled out.

3 Oblique impact experiments and results

The fracture/fragmentation behavior of the AP projectile was studied in a series of inclined impact experiments. The details of the experiments are provided in Table 2 and the

Table 2. Details of oblique impact experiments.

Config. #	Plate thickness (mm)	Obliquity angle (deg.)	Areal weight (kg/mm^2)
1	3.2	49	38.3
2	4.2	49	50.2
3	5	49	59.8
4	5	35	47.9
5	6	35	57.5

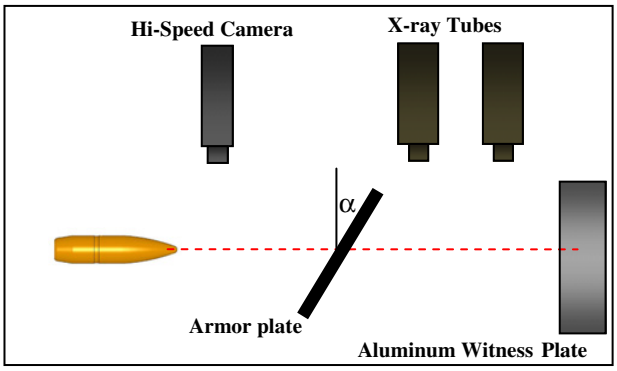

Fig. 2. Schematic view of set-up of oblique impact experiments.

experimental set-up is shown in Figure 2. The experiments were equipped with two high-speed cameras and two x-ray tubes. The fragments of the projectiles were caught in the 40-mm thick aluminum witness plate. High hardness (~500 BHN) armor steel plates of 3.2 to 6 mm nominal thickness were subjected to oblique impact of the projectile at a velocity of 930 ± 10 m/sec. Two shots were executed for each configuration listed in Table 2. Figure 3 displays the x-ray images recorded in the impact experiments with an obliquity angle of 49 degrees. The left hand column of x-ray images corresponds to 108 μsec after impact; the right hand column corresponds to 540 μsec.

According to the x-ray image in Figure 3(a) (3.2 mm thick steel plate) the core was fragmented into two main parts, "nose" and "tail", and few smaller fragments from the middle of the core.

Increasing the thickness of the steel plate to 4.2 mm (Figure 3(b)) resulted in the fracturing of the core to 3-4 large and many smaller fragments. A further steel plate increase in thickness to 5 mm caused the core to shatter to many medium and small fragments. As the angle of obliquity and strength of the steel plate are parameters which may be associated with the amplitude of the asymmetric loads applied on the core, the thickness of the plate seems to be a factor which controls the duration of the loads. It seems that in the first instance the thickness (3.2 mm) and, therefore, the duration of the asymmetric loads, are insufficient to cause multiple fractures. Figures 4(a-d) display the x-ray images recorded in the impact experiments with an obliquity angle of 35 degrees. Examination of the x-ray images recorded at 540 μsec after impact reveals that an increase of steel plate

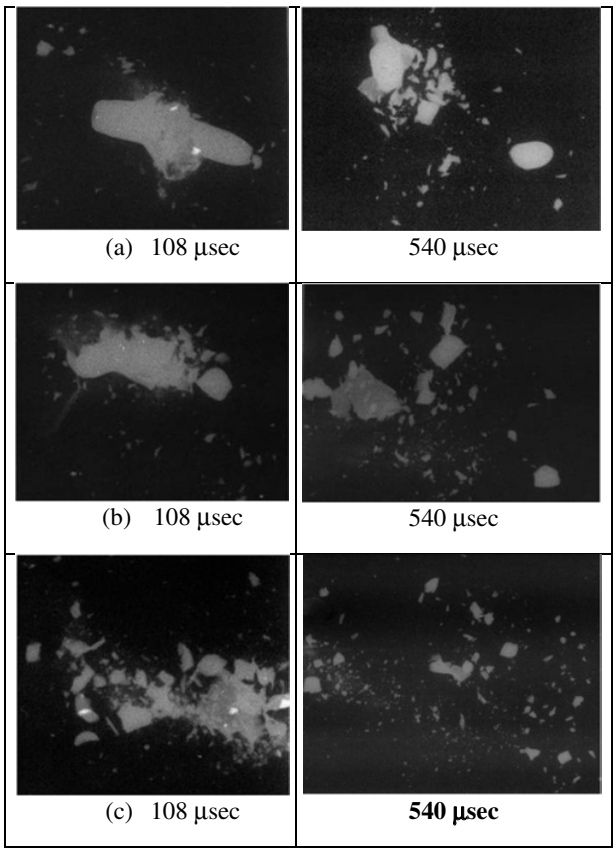

Fig. 3. X-ray images of the 14.5 mm AP projectiles after perforation of high hardness steel plates inclined at 49 deg. Plate thicknesses are as follows: (a) 3.2 mm, (b) 4.2 mm and (c) 5 mm.

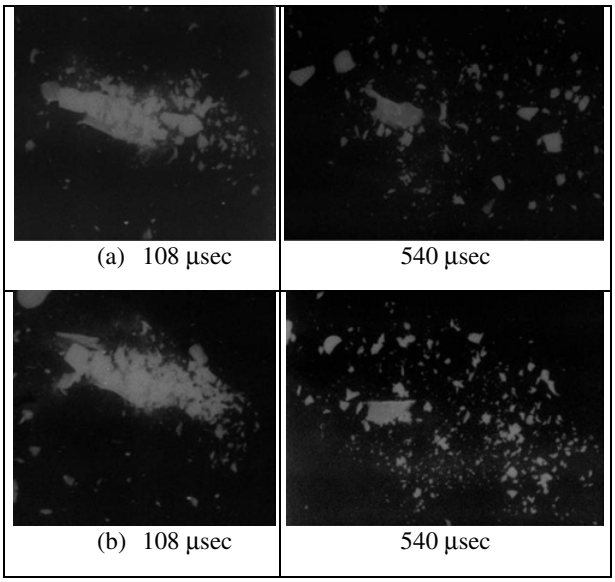

Fig. 4. X-ray images of the 14.5 mm AP projectiles after perforation of high hardness steel plates inclined at 35 deg. and of the following thicknesses: (a) 5 mm; (b) 6 mm.

thickness from 5 to 6 mm resulted in the shattering of the core into smaller fragments. Again, increased duration of the asymmetric loads is believed to be responsible for a more significant level of fragmentation in the tests with 6 mm thick plates.

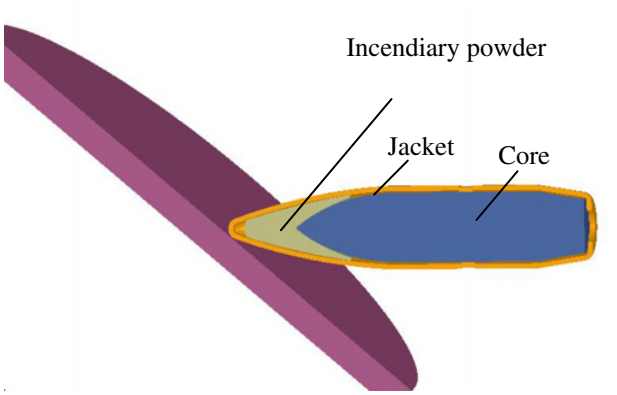

Fig. 5. FE model configuration: 5 mm thick HH steel plate impacted at 49 deg. of obliquity.

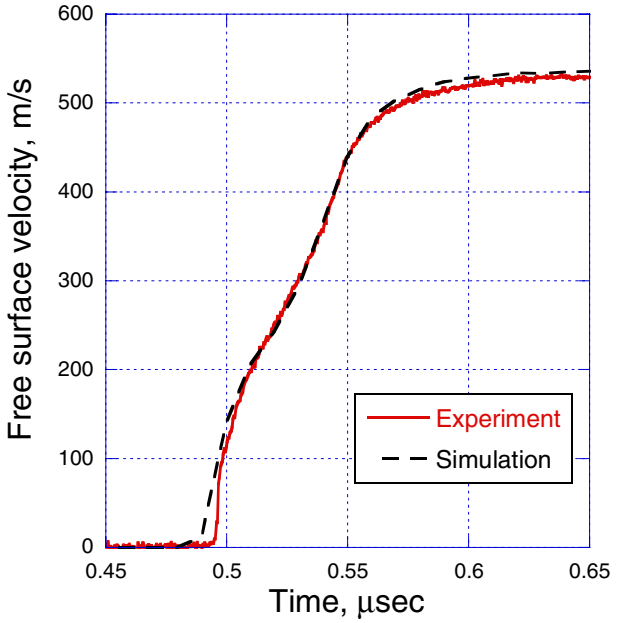

Fig. 6. Free surface velocity profile recorded in planar impact experiment (BALA) along with the profile obtained in FE simulation.

4 Numerical simulations and results

4.1 The FE model

Commercial finite element code LS-DYNA was used for modelling of the oblique impact experiments described in the previous section. Due to the symmetry of the problem, a half-space model was used. In addition, instead of modelling a full-sized plate, only a circular plate segment of 100 mm diameter was used in the simulations. The target in the area adjacent to the impact point and projectile components were modelled with brick elements having an average dimension of about 0.5 mm. The finite element model is shown in the Figure 5.

4.2 Materials modelling and results

The Johnson-Cook constitutive relation was chosen to model the projectile core material strength [6]. Here the

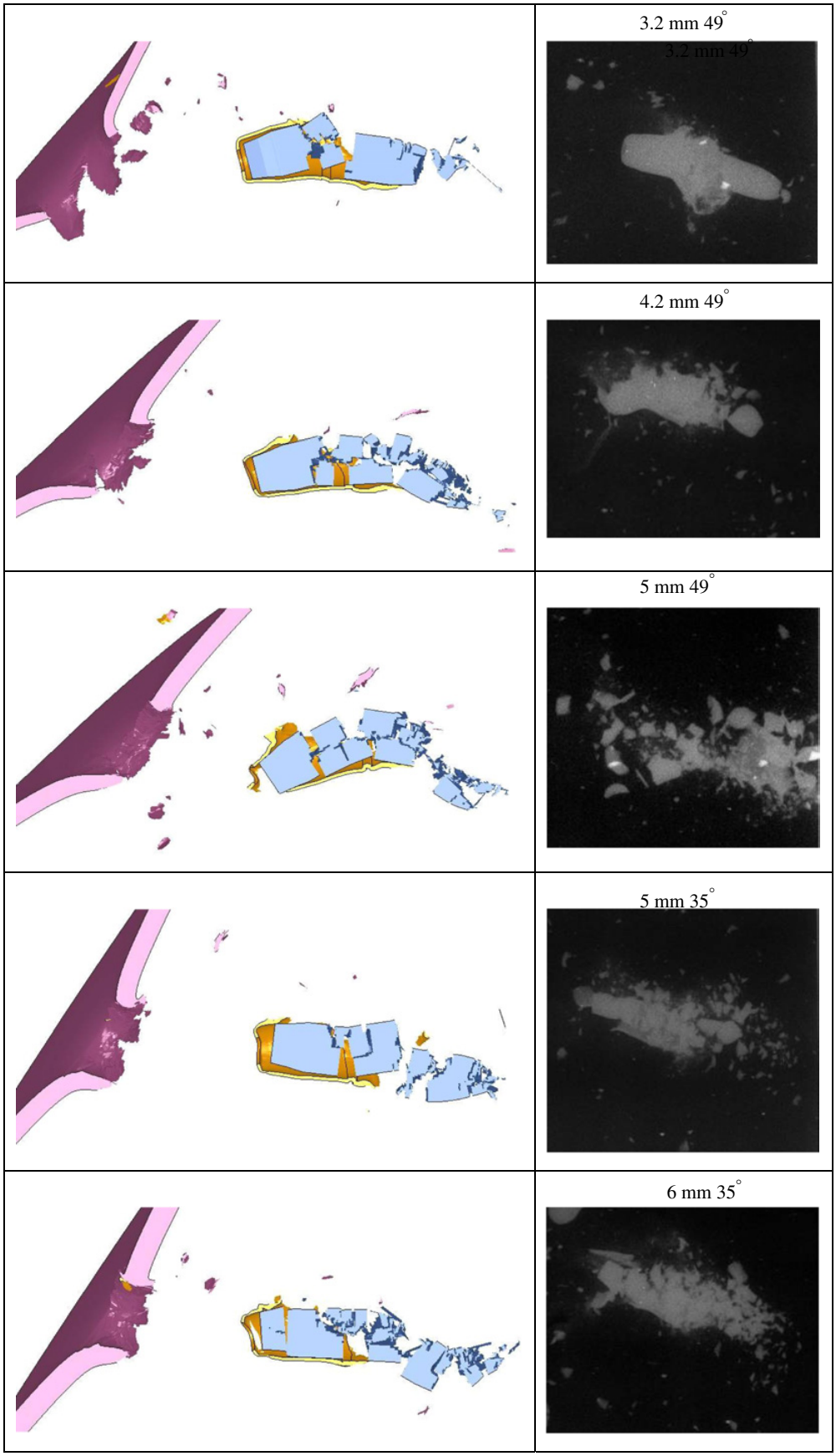

Fig. 7. Fragmentation patterns obtained in the simulations (left side) and in the experiments (right side) of the oblique impact.

Table 3. Material constants for the steel of the 14.5 mm API core.

Elastic constants and density			Yield strength and strain hardening			Strain rate hardening		Temperature softening			Failure	
ρ_0, g/cm^3	G, GPa	E, GPa	A, MPa	B, MPa	n	C	$\dot{\varepsilon}_0$, 1/s	M	Tm, K	Cp, J/kg×K	Spall type	σ_p, MPa
7.79	79.3	205	1400	9000	0.35	0.03	1	1.0	1793	477	2	2600

equivalent strength is expressed as

$$\sigma_{eq} = \left(A + B\varepsilon_{eq}^{n}\right)\left(1 + \dot{\varepsilon}_{eq}^{*}\right)^{C}\left(1 - T^{*m}\right) \qquad (4)$$

where ε_{eq} is equivalent plastic strain and A, B, n, C and m are material constants. The dimensionless plastic strain rate is given by $\dot{\varepsilon}_{eq}^{*} = \dot{\varepsilon}_{eq}/\dot{\varepsilon}_0$, where $\dot{\varepsilon}_0$ is a reference strain rate. The homologous temperature is given by $T^* = (T - T_r)/(T_m - T_r)$ where T is the absolute temperature, T_r is the room temperature and T_m is the melting temperature. Fracture of the core material is modelled using the principal tensile stress failure criterion. The compression part of the calculated and measured free surface velocity profiles of planar impact test BALA are shown in Figure 6. The parameters A, B, n and C of the Johnson-Cook constitutive relation were obtained by matching the free surface histories measured in planar impact tests to calculated histories. Linear thermal softening was assumed for the core material, $m = 1$. The maximum principal tensile stress spall model was used to describe the brittle failure of the core material. This criterion is implemented using the SPALL parameter where option 2 is chosen. According to plate impact results, spall strength of about 3-3.8 GPa was measured for the core steel. However, these values were found to be too high for capturing the failure behavior of the core in the simulations. Several values of the principal tensile stess limit σ_p were checked by matching the modelled fracture patterns to x-ray images. Although x-ray images of the projectile after perforation of a steel plate at normal incidence are not in our possession, according to our experience in such scenarios, the core should remain intact. Therefore, the lower limit for the value of maximum principal tensile stress (2.5 GPa) was dictated by keeping the core unfractured at normal incidence impact.

A series of iterative simulations with σ_p in the 2.5-3 GPa range was carried out. A value of 2.6 GPa was chosen as a compromise in order to address the range observed in the fracture behavior of the 14.5 mm API core. The ADD_EROSION model of LS-DYNA was used to dispose of the failed elements which reach a tensile volumetric strain of 10% thereby allowing visualization of the fractures. The material constants for the core steel are given in Table 3. The constitutive behaviors of the jacket steel and of the incendiary powder were described with simplified Johnson-Cook model (MAT098) [7]. A modified version of the Johnson-Cook model was chosen for the description of the strength and failure of the high hardness armor steel [8]. The parameters of the models for the jacket, incendiary powder and the armor steel were taken from our materials database.

Figure 7 demonstrates the fragmentation patterns obtained in the simulations of oblique impact experiments along with respective x-ray images taken at 108 μsec after impact. The simulated fracture pattern of the core with

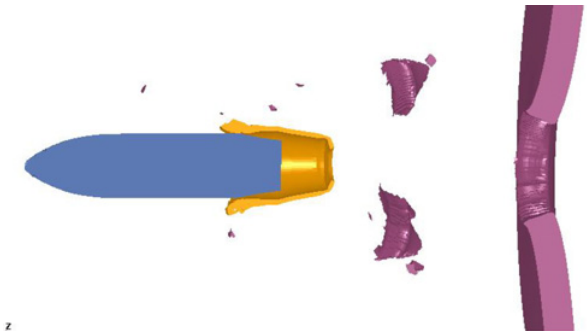

Fig. 8. Fragmentation pattern obtained in the simulations of the impact at normal incidence. No fracture of the core was observed.

3.2 and 4.2 mm steel plates agrees quite well with the x-ray images (Figures 7(a) and 7(b)). For thicker plates of 5 and 6 mm, the similarity of the modelled and experimental fragmentation patterns is not as impressive. The rear part of the core is less fragmented than was predicted by the x-ray analysis. However, the trend obtained in degree of fragmentation in the simulation is the same as that received in the x-ray images. One can state that fragmentation pattern could be mesh-size dependent. This was checked in the course of the simulations by comparison to the pattern obtained with refined mesh (0.25 mm). Indeed, more fragmentation will be obtained with refined mesh and the same set of material constants but it affects all the cases including those where a good match with x-ray results will be lost.

The inability to accurately match the x-ray images for cases with 5 and 6 mm thick plates may be attributed to the simplified description of the spall failure model that was used. In reality, the fracture stress may be strain-rate dependent. As a result, the rear part of the core, which is loaded at a much lower strain rate than the core's nose, may fracture under lower tensile stresses. In addition, the hardness of the surface layer and of the bulk of the core might be different thereby inducing more complex fracture behavior. Figure 8 demonstrates the condition of the projectile as obtained in the simulation of normal incidence impact with the constants from Table 3. The core remains intact as expected in such a scenario.

5 Conclusion

The high strain rate strength and failure behavior of the steel core of 14.5 mm AP projectile have been studied in planar impact tests and oblique impact ballistic tests. From the planar impact tests, the HEL of about 2.3 GPa and the spall strength of 3-3.8 GPa have been determined. According to x-ray records of oblique impact experiments, fragmentation patterns of the core were found to be dependent on both the angle of obliquity and the thickness

of the steel armor plate. A Johnson-Cook strength model with parameters based on planar impact results coupled with a principal tensile stress spall model were used to match the x-ray fragmentation patterns of oblique impact experiments. Even though the simple spall fracture model was not able to catch all the peculiarities in the fragmentation behavior of the core, reasonable agreement between experimental and simulated results was obtained.

Acknowledgements

The authors would like to acknowledge Prof. E. Zaretsky from Ben-Gurion University of the Negev for performing the planar impact experiments.

References

1. Y. Yeshurun, Z. Rosenberg. AP projectiles fracture mechanisms as a result of oblique impact. In: Murphy MJ, Backofen JE, editors. Proceedings of the 14th international symposium on ballistics. 537 (1993)
2. L.M. Barker and R.E. Hollenbach. Laser interferometer for measuring high velocities of any reflecting surface. J. Appl. Phys.; **43**: 4669 (1972).
3. S Jacobi, E.B. Zaretsky and D. Shvarts. Experimental Examination and Numerical NAG Model Analysis of Spall Sensitivity to Microstructure in Copper, J. Phys. IV.; **10**: 805 (2000)
4. L. M. Barker and R. E. Hollenbach, Shock Wave Study of the $\alpha \rightleftarrows \varepsilon$ Phase Transition in Iron, J. Appl. Phys. 45, 4872 (1974).
5. E. B. Zaretsky, Shock Response of Iron between 143 and 1275 K, J. Appl. Phys. **106**, 023510 (2009).
6. W. H. Johnson, G. R. Cook. A Constitutive Model and Data for Metals Subjected to Large Strains, High Strain Rates, and High Temperatures. Proceedings of the 7th International Symposium on Ballistics, 547, (1983)
7. LS-DYNA 971 Ver. 5 keywords manuals, LSTC, (2011).
8. T. Borvik, O.S. Hopperstad, T. Berstad, M. Langseth. A computational model of viscoplasticity and ductile damage for impact and penetration. Eur. J. Mech. Sol. **5** (2001)